atmosphere

MDPI

Article

Modelling Cyclists' Multi-Exposure to Air and Noise Pollution with Low-Cost Sensors—The Case of Paris

Jérémy Gelb and Philippe Apparicio *

Institut National de la Recherche Scientifique, Centre Urbanisation Culture Société, Montréal, QC H2X 1E3, Canada; jeremy.gelb@ucs.inrs.ca

* Correspondence: philippe.apparicio@ucs.inrs.ca

Received: 5 March 2020; Accepted: 19 April 2020; Published: 22 April 2020

Abstract: Cyclists are particularly exposed to air and noise pollution because of their higher ventilation rate and their proximity to traffic. However, few studies have investigated their multi-exposure and have taken into account its real complexity in building statistical models (nonlinearity, pseudo replication, autocorrelation, etc.). We propose here to model cyclists' exposure to air and noise pollution simultaneously in Paris (France). Specifically, the purpose of this study is to develop a methodology based on an extensive mobile data collection using low-cost sensors to determine which factors of the urban micro-scale environment contribute to cyclists' multi-exposure and to what extent. To this end, we developed a conceptual framework to define cyclists' multi-exposure and applied it to a multivariate generalized additive model with mixed effects and temporal autocorrelation. The results show that it is possible to reduce cyclists' multi-exposure by adapting the planning and development practices of cycling infrastructure, and that this reduction can be substantial for noise exposure.

Keywords: cyclist; exposure; multi-exposure; noise; air pollution; NO_2; Bayesian modelling; spatial analysis; Paris

1. Introduction

Environmental noise and air pollution are two growing issues in cities. Their impacts on health and population well-being are now widely acknowledged. In its latest report on environmental noise in Europe, the World Health Organization (WHO) recognized it as one of the main environmental risks in cities. Two types of health impacts are distinguished: the auditory effects (hearing loss and tinnitus) and non-auditory effects linked to annoyance and stress generated by exposure to noise (physiological distress, disturbance of the organism's homeostasis, increasing allostatic load, sleep loss, concentration difficulties, etc.) [1–5]. The latter are important if the exposure is chronic and prolonged.

For example, the WHO guideline development group identified two priority health outcome lines of evidence for the road traffic noise. The first threshold value of 53.3 L_{den} corresponds to an absolute risk of 10% for the prevalence of a highly annoyed population. The second one of 59.3 dB L_{den} corresponds to an increase of 5% of the relative risk for the incidence of ischemic heart disease [3].

The case of air pollution is more complex because air pollutants are numerous. Research distinguishes gaseous pollutants and vapors (e.g., NO_2, O_3, CO_2, CO, COVs, etc.) from particulate matter (fine: $PM_{2.5}$ and coarse: PM_{10}). The health impacts of these pollutants are numerous: nausea, breathing difficulties, skin and respiratory tract irritations, development of certain types of cancer, birth defects, delayed development in children, reduced immune system activity, etc. [6]. The WHO identifies nitrogen dioxide (NO_2), particulate matter (fine: $PM_{2.5}$ and coarse: PM_{10}), ozone (O_3), and sulphur dioxide (SO_2) as the pollutants with the strongest impact on health. For NO_2 (measured in

this study), the WHO advises not exceeding a mean value of 200 µg/m^3 in an hour, as exposure above this level causes significant inflammation of airways [7].

1.1. Cyclists' Exposure and Transport Justice

Cyclists are particularly exposed to these pollutions. Indeed, they do not have a cabin or an air conditioning system to protect them. A considerable body of literature has compared the levels of exposure to air pollution according to the mode of transportation. Studies have concluded that the differences in terms of exposure are inconsistent [8]. However, when the ventilation rate is taken into account, it is clear that cyclists inhale more air pollutants than other road users. In a recent literature review, Cepeda et al. [9] have found that car users inhaled an average of only 16% of the total dose inhaled by cyclists for similar trips. Less information is available for exposure to noise, but Okokon et al. [10] have found that, on average, cyclists are exposed to 6 more dB(A) than car users in Helsinki (Finland), and 4.0 in Thessaloniki (Greece), on average for similar trips, and Apparicio et al. [11] have found a difference of 1.92 ($L_{\mathrm{Aeq,1min}}$) in Montreal (Canada).

The second main cause of cyclists' overexposure is their direct proximity to a major source of air and noise pollution, i.e., road traffic. This proximity is reinforced by planning policies encouraging road sharing. In Paris, this is striking when one observes the development of the bicycle network [12]. In 2001, the city permitted cyclists to use bus lanes and in 2010, many one-way streets were opened to cyclists in both directions (Figure 1). These two breaks represent major increases in available cycling infrastructures, but this raises the question of the quality of these infrastructures and the closeness to traffic that they entail.

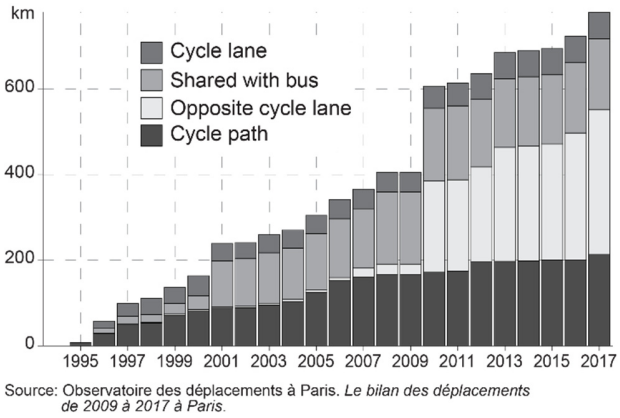

Figure 1. The development of a cycling network in Paris between 1995 and 2017.

Cyclists' overexposure supports the statements of Gössling [13] on transportation justice. The bicycle is a durable mode of transport and helps to reduce congestion, environmental noise, emission of greenhouse gas, and health costs. Yet only a minor portion of the space dedicated to transport is used for cycling infrastructure, and cyclists are overexposed to urban nuisances.

Unfortunately, the problem of cyclists' exposure is rarely considered in the current planning of cycling infrastructure. The London Quietways, which provide cyclists with routes that are quiet and far from traffic [14], constitute an inspiring example which deserves special mention. Yet, new studies suggest that the risk induced by air pollution could be higher than that of road accidents. As an example, Künzli et al. [15], using cohort data, have attributed twice the number of deaths to air pollution in comparison to road accidents in Europe. More specifically, in Paris, Praznoczy [16] has found that the risks associated with exposure to air pollution are considerably higher than those from road accidents. Nonetheless, they conclude that all these risks remain small in comparison with the health benefits of the physical activity of bicycling, and this is supported by Cepeda et al. [9] and De Hartog et al. [17]. Unfortunately, to our knowledge, this type of study does not consider exposure to noise. The current situation is summarized in Figure 2.

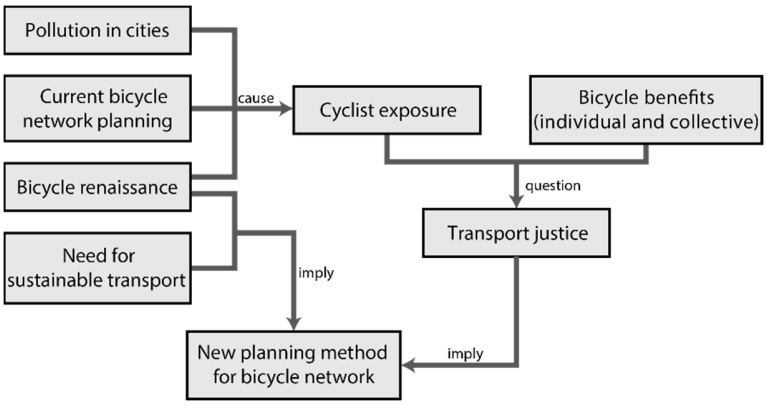

Figure 2. The situation of bicycles in cities.

Cities are potentially characterized by high levels of exposure to air and noise pollution which, combined with the current bicycle renaissance and the lack of cycling infrastructure, lead to a situation where cyclists are overexposed. When considering the collective benefits of urban cycling (a durable mode of transportation, and a reduction in health costs and congestion), this reveals an injustice in transport. The combination of this injustice, the cycling renaissance, and the requirement for sustainable transportation in our society today suggests a need to rethink our practices in cycling infrastructure planning.

This necessitates including the question of cyclists' exposure to air and noise pollution in planning and working to understand how we can reduce these exposures. Many studies have already tried to identify the factors contributing to cyclists' exposure to air or noise pollution [18–20], but there are significant limitations to their scope and generalization potential: few consider noise; the amount of data is limited; there needs to be replication on specific axes; there is no unbundling of background pollution; statistical methods omit pseudo-replication, etc.

1.2. The Development of Low-Cost Sensors: New Paradigm and Opportunities

During the last decade, the development of new technologies and low-cost sensors to measure air and noise pollution has presented opportunities to study these pollutants. The low-cost sensors (in contrast with traditional monitoring network) have drawn attention from research and institutional fields, and in 2013, the EPA proposed a classification with five tiers of sensors to evaluate their potential use and reliability [21]. The first and second tiers are the most limited sensors, mainly built for citizen use and community groups for personal and education purposes. The third and fourth tiers group more accurate devices used to provide complementary data (with higher space-time resolution) to the traditional monitoring networks at a lower cost. Finally, the fifth-tier group reference sensors that are the most reliable and sophisticated but less accessible. The frontiers between these categories are fuzzy, but the low-cost designation applies to the first three tiers. Snyder et al. [22] see in this development the rise of a new paradigm in the measure of atmospheric pollution (this holds true for noise pollution) and distinguish four potential uses for these low-cost sensors: (1) supplementing routine ambient air monitoring networks, (2) expanding the conversation with communities, (3) enhancing source compliance monitoring, and (4) monitoring personal exposure. Morawska et al. [23] realized a comprehensive review of scientific and grey literature using these low-cost sensors. They concluded that manufacturers do not evaluate these sensors' reliability and accuracy with enough care. As a consequence, many research teams started to do this work and some of them report satisfactory agreement levels with reference sensors when the data are pre- and post-processed. As an example, the EPA [24] started a program to evaluate 30 sensors without a calibration process. Low-cost sensors will never replace reference devices, but they offer the opportunity to collect complementary data at much finer space and time scale because of their affordability, ease of use, and small size [25].

This evolution is a driving force in the research field on cyclists' exposure to air and noise pollution. Thus, new tools have been made accessible to researchers to address new research goals like estimating the difference in exposure for similar trips according to the transport mode [9,26], measuring the short term health impact of cyclists' exposure to air pollution [27], or modelling and predicting cyclists' exposure in urban environments [18–20,28,29].

Our study continues this research trend and investigates more specifically the case of Paris (France). In September 2017, data were collected on cyclists' exposure to noise and nitrogen dioxide (NO_2) by using low-cost sensors. The main goal of the paper is to develop a methodology based on an extensive mobile data collection using low-cost sensors to determine which factors of the urban micro-scale environment contribute to reduce cyclists' multi-exposure and to what extent.

2. Conceptual Framework for Modelling Cyclists' Multi-Exposure

To answer this research question, we propose the conceptual framework illustrated in Figure 3.

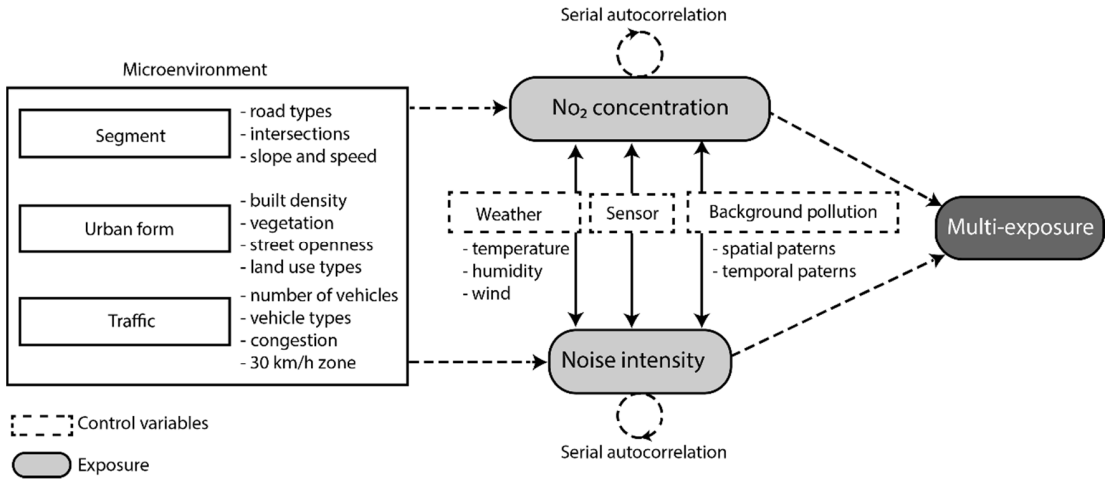

Figure 3. Conceptual framework.

Cyclists are simultaneously exposed to noise and air pollution, measured here as the concentration of NO_2 ($\mu g/m^3$) and noise level (dB(A)). These two exposures depend on the characteristics of the micro-scale-environments through which they travel and the background pollution. The latter follows temporal and spatial patterns. Weather has a direct impact on noise propagation and on NO_2 chemical interactions and dispersion. Finally, the sensors used have a systematic variability in their measurement that has to be controlled. Micro-scale-environment depicts a distinction of the more classical concept of micro-environment in exposure studies. It describes "an individual volume or an aggregate of locations, or even activities within a location [...] hav[ing] an homogeneous concentration of the pollutant being evaluated" [30], such as home, workplace, in-public transport, cycling etc. As we need a more disaggregated and geographical perspective, we define in this study the micro-scale-environment as a chunk of space and time with a homogeneous concentration of pollutants.

Some studies have already investigated the characteristics of the urban environment which might have an impact on NO_2 concentration or noise level. These works are inspired by the classical Land Use Regression (LUR), usually applied to data collected by static monitoring stations [31]. The factors most often considered are as follows:

First, road traffic might be measured as real time traffic recorded specifically during the time span of the study [32,33], estimations of daily traffic volume [34–36], or the type of roads taken by the cyclist [19,28,29]. In all cases, road traffic is associated with cyclists' greater exposure to air and noise pollution.

Second, vegetation is integrated in studies as the number of trees around the samples [19,36], the presence of a park [20,35–37], or its density [34]. The results remain inconsistent and the role of

vegetation in the absorption and deposit of air and noise pollution seems to be small in comparison with the "park effect" induced by the increased distance from pollution sources. In some cases, the vegetation could even retain and trap air pollution (notably in urban canyons) preventing its vertical dispersion [38].

Third, land use, i.e., the density of residential, industrial, and commercial areas, open spaces, and the diversity of land use are indicators generally associated with higher or lower concentration of noise and air pollution. Indeed, neighborhoods with a higher concentration of activities and population accumulate many pollution sources [33,35,36] and, thus, higher levels of pollution are more likely to be observed there.

Fourth, urban morphology, i.e., the build density, street canyons, wind permeability, or the density of intersections are factors describing the geometry of the city and might play an important role in air pollution trapping (canyon effect) and noise propagation [39–41].

3. Material and Methods

3.1. Case Study

Paris is an interesting case study for many reasons. First of all, the city has experienced a typical evolution of bicycle use since the 20th century. The bicycle had fallen into disuse at the end of the Second World War and was largely replaced by the car due to the latter becoming more widely available and the disappearance of cycling sidewalks [42]. The bicycle lost its status as a means of transport and was confined to sports and leisure uses. It was only in the 1980s that the bicycle made its comeback in cities as a means of transportation, promoted by the ecological movement and the rising cost of other means of transport. Some authors name this new period the "bicycle renaissance" [43]. In Paris, one can note a new increase in bicycle use at the beginning of the 2000s, after a period of stagnation since 1970. Between 2001 and 2010, the number of daily trips made by bicycle doubled and reached 650,000 trips in central districts (within the city) [44].

Second, Paris is a city with relatively high levels of air and noise pollution. AirParif and BruitParif are two associations charged by the French government with monitoring air and noise pollution, respectively, in the region of Île de France. In its 2017 annual report, AirParif indicates that, over 6 days, the O_3 and particulate matter concentrations exceeded the fixed threshold (for a total of 12 days). The association estimates that 1.3 million residents in the region are exposed to NO_2 concentration levels higher than the standard for annual exposure and that 10 million are living in places where the French quality standard for annual exposure to $PM_{2.5}$ (10 $\mu g/m^3$) is exceeded. The proximity to road traffic appears to be the main source of pollution in the report [45]. The maps of annual NO_2 concentrations (available in the document [45]) depict a clear gradient from central to outlying areas. This phenomenon is explained by the higher density of activities, population, trips, and equipment and a more densely built environment, less favorable to air pollution dispersion.

In 2017, BruitParif [46] estimated that only 15% of the region's population living in dense urban areas was exposed to annual daily mean levels of noise below 53 dB(A) (the WHO guideline) and 11% was exposed to levels higher than 68 dB(A) (the intervention threshold defined by the European Union). Overall, 65,607 years of healthy life expectancy are lost annually in the region because of noise exposure. Again, maps are available in the report [46] and transport (air, rail, and road transport) appears to be the main source of this problem.

Therefore, in this context where the number of cyclists is increasing and the levels of exposure to air and noise pollution are potentially high, a study on cyclists' multi-exposure is clearly justified.

3.2. Primary Data Collection and Structuration

Primary data was collected in Paris over four days in September 2017 (4 September to 7 September). Three participants (two graduate students and one professor) cycled approximately 100 km every

day between 08:00 a.m. and 6 p.m. This study has been approved by the Institutional Review Board (Ethical Review Board of Institut national de la recherche scientifique) (Project No CER-15-391).

We realized a mobile data collection using portable low-cost sensors to measure the exposure on three participants. This research falls within the new paradigm of data collection on individual exposure. Indeed, classical monitoring networks have been found to be not very representative of individual exposure [47,48]. This can be explained by the low density of their spatial coverage that fails to measure the micro-variations of pollution in urban areas [49–51]. Moreover, these stations are generally not located directly on streets, but some meters above the ground or on the top of buildings, which contributes to an underestimation of people's direct exposure at road level [47,52,53]. MacNaughton et al. [34] reports values for NO_2 (ppb) of 24.2 ppb measured by mobile sensors (sampled concentration) versus 15.9 ppb by static stations (background pollution) on a designated bike lane. Different authors likewise observed higher variations for other pollutants [20,54,55].

The use of low-cost sensors and a mobile approach has several drawbacks. First, because of its ephemeral nature, the mobile data collection is not suited for an assessment of seasonal variations of pollution. This could be achieved by repeated and periodic data collection but with a significant increase of the costs. This type of question must preferably be investigated with data collected from traditional monitoring networks. Second, this approach produces less reliable measurements and might not provide an accurate estimation of typical values of pollution concentrations on specific streets. To overcome these limitations, Van den Bossche et al. [47] and Hatzopoulou et al. [56] propose an intensive approach based on repetitive sampling of the same segments. The repetition of measurement is a way to compensate for the considerable variability of the data and the lower accuracy of the sensors. However, this method limits the spatial coverage of the study area and, thus, the diversity of sampled environments, which is one of the main appeals of the use of low-cost sensors combined with mobile data collection. Therefore, we propose an extensive approach (in opposition to an intensive approach), aiming to maximize the spatial coverage and the diversity of environments travelled. The goal is not to estimate precisely the expected values of exposure to pollution on a specific segment (which is difficult with low-cost sensors), but rather to understand the impacts of urban environmental characteristics in their (almost) full range of values on individual exposure. A similar approach has already been applied successfully in Ho Chi Minh City (Vietnam) [57], Portland (Oregon, USA) [35], Ghent (Belgium) [40], Flanders (Belgium) [58] (even if the expression "extensive data collection" was not used). The replicability of the study is not affected by this design. Indeed, the trips are recorded and could be replicated. Obviously, the exact conditions of traffic and meteorology cannot be reproduced, but this is also true for the intensive design.

The trips were defined before the data collection with GoogleMaps and stored with MyMaps. During the data collection, the participants had to follow the routes on their smart phone fixed on the handlebar and to modify them in case of perturbation (closed street, road work, stairs, etc.). Following the extensive design approach, the trips were chosen to maximize the spatial coverage and the diversity of urban environments, and to reduce repetitive samples on the same segments.

To measure the nitrogen dioxide (NO_2) concentration ($\mu g/m^3$), temperature (°C), and humidity (%), participants were equipped with an Aeroqual Series 500 Portable Air Quality monitor (Aeroqual Limited, Auckland, New Zealand) and its two sensors (one for NO_2 concentration and one for temperature and humidity). This device has a temporal resolution of 1 min. According to the Aeroqual supplier's product information, the NO_2 sensor has the following characteristics: range (0–1 ppm), minimum detection (0.005 ppm), accuracy of factory calibration ($<\pm 0.02$ ppm 0–0.2 ppm; $<\pm 10\%$ 0.2–1 ppm), and resolution (0.001 ppm). The sensors used were new and thus pre-calibrated by the supplier. As recommended by the fabricant, we let them run during 24 h the day before the data collection, and 1 h (warmup) every morning before starting the trips. The device was fixed to a harness on the right shoulder of the participant, as close as possible to the breathing area. The Aeroqual NO_2 sensor is known for its cross-sensitivity to O_3 [59], and the risk is to overestimate the concentration of NO_2 in the presence of O_3. However, filtering out the O_3 concentration from the recorded values leads to a

strong linear relationship with reference analyzer [60]. No O_3 sensor was available during this data collection, but we propose another approach based on statistical methods to control its contribution to the measurements (see Sections 3.3 and 5.1). Aeroqual Series 500 monitors have largely been used in numerous studies on individual exposure or air pollution mapping, e.g., [11,19,61–63].

To measure noise level ($L_{Aeq,\ 1min}$, dB(A)), a Brüel and Kjaer Personal Noise Dose Meter (Type 4448, class 2, conform to IEC 61252:2002 and ANSI S1.25:1991 standards) was fixed on the participant's left shoulder (as recommended by the manufacturer) facing the road with their wind-shield. This device has a temporal resolution of 1 min and has the following characteristics: exchange rate (3 dB), sound level range (certified 65–140 dB, reliable down to 58 dB), accuracy (±2 dB). This device does not record the frequency spectra. As recommended by the manufacturer, the Personal Noise Dose Meters were calibrated once a day using the Sound Calibrator Type 4231 (calibration accuracy ±0.2 dB). Triathlon GPS watches (Garmin 910 XT) were used to record the GPS track of the trips with a temporal resolution of 1 s. Finally, action cameras (Garmin Virb XE) fixed to the handlebar were used to record videos of the trips.

More recent sensors of noise and air pollution however offer a lower temporal resolution, but at higher variability cost in the collected data. A temporal resolution of 1 min is sufficiently detailed considering that with a mean speed of 15 km/h, a cyclist can ride only 250 m.

The GPS tracks were map-matched to the Open Street Map (OSM) road network using the algorithm OSRM [64]. This data structuration step was validated manually by using videos of the trips. The traces were cut as 1-min segments (temporal resolution of the sensors) and all the measurements were assigned to these segments by using timestamp (the clocks of each device were synchronized every morning during the data collection). The OSM street network dataset was selected rather than the official city network because, the OSM network nomenclature is common to each city in the world and thus will allow easier comparisons between papers using this dataset in this field study [57]. Only 5% of the sampled segments were not categorized or not present in the database and were thus classified as "unclassified roads". Apart from missing data, OSM is criticized for inaccuracy in the road typology, notably for roads smaller than primary roads [65]. According to the same work, the quality of the OSM data increases with the density of contributors, and they are numerous in big cities like Paris. A more recent study concludes that "the Paris OSM road network has both a high completeness and spatial accuracy [. . .] and is found to be suitable for applications requiring spatial accuracy up to 5–6 m." [66]. This level of accuracy is appropriate for our study. The data was not pre-processed before data analysis. Only the observations with missing values or measurements exceeding the measurement ranges were removed.

3.3. Data Analysis—Building a Model to Estimate the Impact of Micro-Scale Environment

Let us recall here that the main goal of this study is to identify the factors of the micro-scale-environment that contribute to cyclists' multi-exposure and to evaluate the extent of these contributions. The most used method to achieve this goal is regression analysis, with the exposure measurements as dependent variables. However, the use of low-cost sensors combined with the mobile extensive data collection design raises many methodological challenges in the analysis of the data.

First, we must deal with the problem of pseudo-replication. Indeed, two factors violate the condition of independence of observations: the day of data collection and the sensor. Day to day, because of specific weather and/or traffic conditions, exposure values might vary systematically (part of background pollution). In the same manner, two observations coming from the same sensor are more likely to be similar than two observations coming from different sensors (sensor effect). Hence, the day of data collection and the sensors are incorporated in the models as random effects because they impose a hierarchical structure on the dataset (grouping effect), and thus allows us filter out these effects from the data.

Still with regard to pseudo-replication, the temporal autocorrelation has to be controlled. Our data can be seen as a temporal series, so two consecutive observations are more likely to be similar

than two observations selected randomly. This is rarely done in this field study, but it is necessary to obtain unbiased coefficients in the model.

Secondly, the cyclists' exposure measurement combines both the background pollution (structural spatial-temporal variations) and the immediate pollution specific to the micro-scale environment (which is the primary interest in this study). Thus, to estimate the role of the micro-scale environment, it is essential to distinguish them. To do so, some studies propose using external data coming from static stations to adjust the exposure data by subtracting the background pollution [40], or by adding it as a covariate [20,34] in the analysis. Considering the fact that temporal and spatial patterns of background pollution are integral parts of the collected data, we propose instead to model them directly as nonlinear terms [67]. These terms make it possible to capture the systematic variation through space and time of our exposure data and to model the effects of the micro-scale environment, without using Supplementary Data. This method has already been proven to be useful in modelling cyclists' exposure to noise [57]. Nonlinear terms (e.g., splines) are regularly employed to model exposure to air pollution [40,41]. For space, a bivariate spline can be constructed from the coordinates of the sampling segments. In the model, it reflects the systematic spatial variation of noise and NO_2, everything else being equal. Thus, it can be interpreted as the spatial pattern of the background pollution. In the same way, a univariate spline for time can be built from the timestamp of the sampling segment and can be interpreted as the temporal pattern of the background pollution.

Finally, we have to model two dependent variables simultaneously: noise and NO_2 exposures. Considering the fact these two pollutions share some of their sources, it is likely that they share some variance. Thus, we propose to model them simultaneously with a multivariate regression model [68]. Theoretically, this permits us to be closer to the multi-exposure concept. Statistically this model allows to consider a potential correlation between the two dependent variables. The proposed model is detailed bellow:

$$y_z \sim D(\mu_z, \sigma_z) \tag{1}$$

$$\mu_{z[i]} = \alpha_z + \sum_{p=1}^{l} X_{z[i]} * \beta_{zl[i]} + \alpha_{zsens_{[ij]}} + \alpha_{zday_{[id]}} + \sum_{p=1}^{n} f_{zp}\left(X_{[i]}\right) + \sum_{p=1}^{k} \varnothing_p \varepsilon_{zi-p} + \varepsilon_z$$

$$\alpha_{z\ capt} \sim normal\left(0, \sigma_{z\ capt}\right)$$

$$\alpha_{z\ jour} \sim normal\left(0, \sigma_{z\ jour}\right)$$

$$\varepsilon_z \sim normal\left(0, \sum \varepsilon\right)$$

with i an observation (1-min segment),

D a specific distribution (Gaussian or student in this article),

z a dependent variable (NO_2 concentration or noise level in this article),

α the general intercept,

l the number of fixed linear parameters in the model,

j a sensor and d a day of the week,

α_sens a vector of intercepts for each sensor, normally distributed and centered on 0,

α_day a vector of intercepts for each day, normally distributed and centered on 0,

n the number of nonlinear parameters in the model,

f a nonlinear function,

k the maximal lag to consider for the temporal autocorrelation parameter (MA),

The noise vector ε_i for each observation i is jointly normal (and centered on 0), so that the outcomes for a given observation are correlated. The variances of dependent variables are assumed to be constant.

The model above is implemented in a Bayesian framework in R [69] with the package *brms* [70] based on STAN [71]. The used priors are described in Supplementary Material (S1). We fitted the

model using four chains, each with 10,000 iterations where the first 1000 were used as a warmup for sampling realized with a No-U-Turn Sampler (NUTS).

The predictors are described in Table 1. Following the literature review presented above, many terms describing the 1-min segment characteristics (slope, speed of the cyclists, and number of intersections encountered), the road traffic (type of road, type of cycling infrastructure, low-speed zone, and distance to the closest main road), land use (activity density in a 50 m buffer), and vegetation (canopy density in a 50 m buffer) were introduced as independent variables. Two predictors describing the urban form were also used: the percentage of visible sky from the ground (street canyon proxy), the fetch index (indicator of potential local wind exposure), and its interaction with wind. Finally, two covariates describing the weather conditions were added to the model: the temperature (measured by the portable air pollution sensors) and the wind speed (available for each hour from Paris weather stations). Humidity was discarded because of its strong correlation with temperature. Details of the calculations and the data source of each index are available in Supplementary Material (S2).

Table 1. Independent variables included in the regression model.

Dimension	Variable	Type
Micro-environment	Slope (%)	Linear effect
	Cyclist's speed (km/h)	Linear effect
	Number of intersections encountered	Linear effect
	Type of road (proportion of 1 min)	Linear effect
	Low-speed zone 30 (0–1)	Linear effect
	Distance from main road when on cycling infrastructure (m)	Nonlinear effect
	Industrial activity land use density (%) in a 50 m buffer	Linear effect
	Vegetation density (%) in a 50 m buffer	Linear effect
	Sky view factor index (%)	Linear effect
	Fetch index (%)	Linear effect
	Fetch index * wind speed	Linear effect
	Temperature (°C)	Linear effect
	Wind speed (km/h)	Linear effect
Background-pollution	Coordinates (X,Y)	Nonlinear effect
	Number of minutes since 07:00 AM	Nonlinear effect
Control factors	Day of the data collection	Random intercept
	Sensor	Random intercept
	Temporal autocorrelation	MA2 term

4. Results

4.1. Descriptive Analysis

Before presenting the results of the analysis, some descriptive statistics should be reported. A total of 3822 observations of 1-min segments were collected for a total of 64 h and 964 km traveled. Figure 4 is a map of the trips accomplished. This represents an extensive coverage, we calculated that if we divide the intra-muros area of Paris in squares of 250 m length, then we have sampled, at least once, 52% of them.

Table 2 displays descriptive statistics of NO_2 and noise exposure, however, these values must be interpreted with caution. They are raw data coming from low-cost sensors and could overestimate real exposure, especially for NO_2 because of cross sensitivity of the sensor to O_3 (see Section 3.2) and the strong day to day variation. Indeed, we observed a difference of 35 $\mu g/m^3$ between higher (4 September) and lower (3 September) days for NO_2 mean exposure. For time of day, over the same period, the NO_2 concentration recorded by AirParif had a mean of 37.8 $\mu g/m^3$ with 10% of the records below 10 $\mu g/m^3$ and 90% of the records higher than 77 $\mu g/m^3$. A direct comparison of these values is hazardous considering that the locations of the AirParif fixed stations are chosen to reflect regional air concentration, while mobile individual exposure is measured directly in streets. Although

various studies found considerable gaps between regional concentrations and individual exposure obtained during a mobile data collection [20,34,35,72], it is still likely that our sensors overestimate the cyclists' exposure.

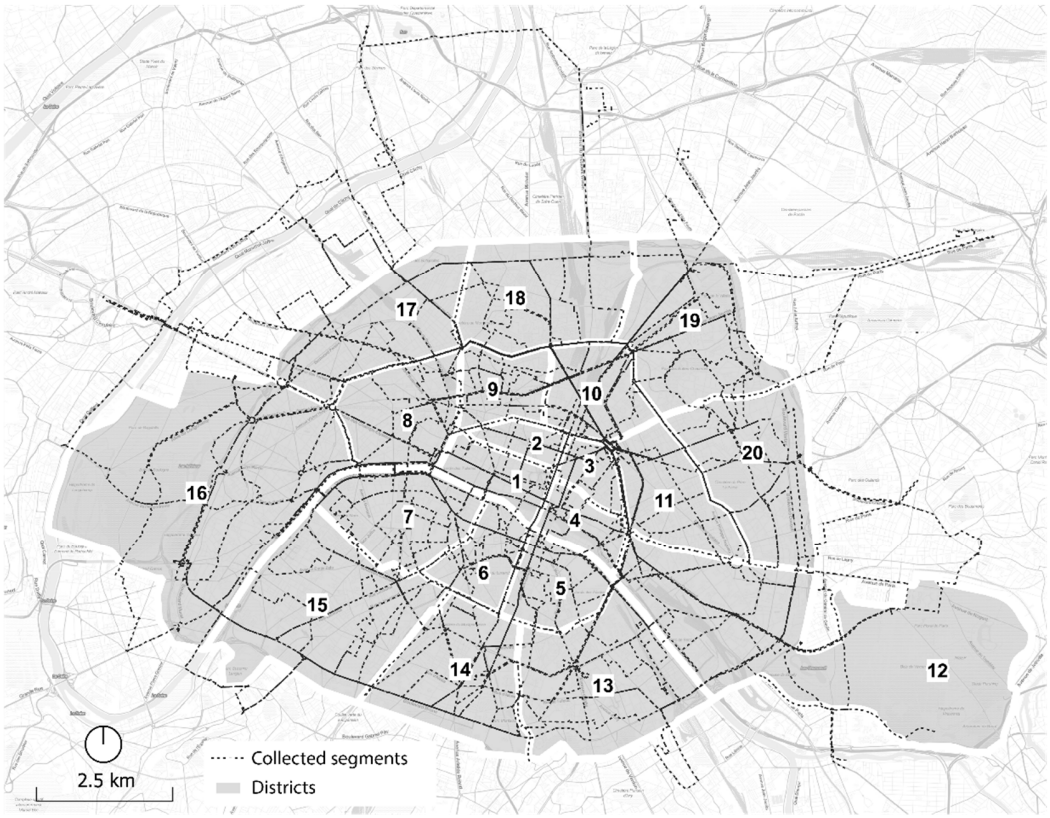

Figure 4. Study area and sample routes.

NO_2 is characterized by a stronger temporal autocorrelation than noise, meaning that consecutive values of NO_2 concentration are more similar than values of noise level. This is explained by the fact that noise is more impacted by short time events like a truck passing, honking, or the crossing of a residential street. NO_2 is less influenced by these events because of its slower dispersion and its accumulation in air. In contrast, the spatial autocorrelation is stronger for noise, meaning that noise exposure is more characterized by spatial structures than NO_2.

Not surprisingly, the correlation between NO_2 concentration and noise level (at the 1-min resolution level) is weak (Pearson: 0.11) and this corroborates previous studies for the same air pollutant [19] or $PM_{2.5}$ [73]. Davies et al. [74] have reported a moderate correlation (0.5) of exposure to NO_2 and noise but their data were collected in less diversified environments and aggregated in 5-min observations (compared to 1 min in our study). Dekoninck et al. [40] suggest in their analysis that air pollution correlates with noise when considering only low frequency noise (caused by engine). This implies to discard all the higher frequency noise produced by honks, breaks, and other events in the urban environment to which the cyclists are also exposed. In our case, the correlation between noise and NO_2 could also be reduced by the measurement error of NO_2 sensors.

Table 3 shows the total time spent on each type of road during the data collection. This information comes from the OSM road network (key *Highway*), and a formal description of each type is available online in the OSM documentation [76].

Table 2. Descriptive statistics for dependent variables.

Statistic	NO_2 (µg/m^3)	$L_{Aeq,\,1\,min}$ (dB(A))
Mean [a]	163.1	72.4
Standard deviation [a]	37.2	4.5
Percentiles		
5	107.2	65.0
10	118.8	66.5
25	137.2	69.1
50	161.4	71.6
75	185.4	74.0
90	209.5	76.0
95	225.6	77.3
99	76.5	78.9
ACF with		
K = 1	0.70	0.61
K = 2	0.54	0.36
Moran I	0.18 (d = 300)	0.31 (d = 200)

Note: to calculate Moran's I statistic, we used a binary matrix and defined as neighbors of the segment *i* all the segments in a buffer of length *d* around *i* with *d* ranging from 50 to 500 m with a step of 50 m. Only the highest values are here reported. [a] Mean and SD of dB values are computed using the *seewave* package [75]. These values are raw data and must be interpreted with care, especially the NO_2 values which probably overestimate the real individual exposure.

Table 3. Time spent on each type of road and cycling infrastructure.

	Total Time	
	Minutes	**%**
Road type		
Primary road	873	22.8
Secondary road	697	18.2
Tertiary road	377	9.9
Residential street	569	14.9
Pedestrian path	105	2.7
Service	208	5.4
Cycleway	802	21.0
Unclassified	191	5.0
On street cycling infrastructure		
Bicycle lane	224	5.9
Opposite lane	106	2.8
Shared bus lane	325	8.5

4.2. Model Adjustment

To build the multivariate regression model, we started with two models in which NO_2 and noise exposures were modelled as bivariate Gaussian distribution and bivariate student distribution to model formally the correlation between residuals. However, we observed that NO_2 and noise did not follow the same type of distribution. A Gaussian distribution was more suited for noise and a student distribution for NO_2 to approximate their respective original distributions. With two different distributions, it is no longer possible to model formally the residual correlation between the two variables, but the latter was weak in the previous models (0.05 for the bivariate student model and 0.04 for the bivariate Gaussian model). Therefore, we decided to keep the model with two different distributions. The graphical posterior predictive checks, which assess the quality adjustment between the original data and the predictions of the model, are available in the Supplementary Material S4. They show that the model is well fitted and managed to reproduce the original distribution of the variables. Note that the values are reported as follows: mean (0.05–0.95 credibility interval).

All models' parameters converged (Rhat = 1.0) and all the trace plots display important mixing (four chains with random start values, with 10,000 iterations, posterior distribution plots are available in Supplementary Material S3). For the NO_2 equation, Bayes R^2 is 0.31 (0.29–0.33) when keeping only

the fixed effects, and 0.54 (0.53–0.56) with the random effects. Respectively, for noise equation, Bayes R^2 are 0.45 (0.43–0.46) and 0.46 (0.44–0.47). Again, the temporal autocorrelation is stronger for NO_2 exposure (MA [1] = 0.57 (0.54–0.60)) than noise exposure (MA [1] = 0.48 (0.45–0.51)), but this effect has been well controlled by the mode because no more spatial or temporal autocorrelations were remaining in model residuals (dB(A) ACF at lag 1 = −0.00, at lag 2 = 0.01, NO_2 ACF at lag 1 = −0.04, at lag 2 = 0.06).

4.3. Controlling for the Background Pollution

To control the background pollution, we introduced different terms in the model. First, we added random intercepts varying by day. The noise exposure varied weakly within days of the data collection (variation lower than 0.5 dB(A), Table 4). For the NO_2 concentration, we noted a lower concentration on Tuesday (on average −29.5 µg/m^3) and higher concentrations on Thursday (on average +15.8 µg/m^3). They represent 18% and 10% of the global average we reported above, respectively. This clearly indicates that NO_2 exposure is more dependent on data collection days rather than noise exposure. This stresses the necessity to include this effect in the model.

Table 4. Model's fixed and random effects.

	NO_2 (µg/m^3)				L_{Aeq} (dB(A))			
	Estimate	**S.E.**	**0.05 CI**	**0.95 CI**	**Estimate**	**S.E.**	**0.05 CI**	**0.95 CI**
Fixed terms								
Intercept	128.65	28.44	72.58	184.56	70.49	2.35	65.83	74.92
Temperature	1.72	0.78	0.22	3.25	0.07	0.09	−0.10	0.25
Wind speed	−0.99	0.54	−2.06	0.08	−0.02	0.07	−0.16	0.13
Fetch index	−0.07	0.06	−0.18	0.05	0.00	0.01	−0.02	0.02
Sky view factor index	−0.06	0.04	−0.15	0.03	0.02	0.01	0.01	0.03
Primary road	Ref.				Ref.			
Secondary road	1.88	1.58	−1.16	5.01	−0.98	0.21	−1.40	−0.56
Tertiary road	−1.24	1.92	−5.02	2.52	−1.88	0.27	−2.40	−1.36
Residential street	−1.05	1.82	−4.66	2.52	−4.08	0.26	−4.58	−3.57
Pedestrian street	−5.68	3.02	−11.57	0.27	−2.72	0.43	−3.57	−1.89
Service road	3.67	2.30	−0.87	8.16	−1.44	0.32	−2.07	−0.80
Cycleway	0.86	1.59	−2.25	3.93	−1.45	0.23	−1.90	−0.99
Unclassified	1.84	2.23	−2.53	6.19	−2.72	0.31	−3.33	−2.10
Cycle lane	−0.82	1.98	−4.68	3.04	0.40	0.28	−0.15	0.94
Opposite cycle lane	−0.43	2.83	−5.99	5.14	−0.63	0.40	−1.42	0.15
Shared road	−5.75	9.67	−24.53	13.14	0.09	1.88	−3.58	3.78
Shared with bus lane	0.97	1.68	−2.30	4.22	0.52	0.23	0.06	0.97
Low-speed zone 30	−1.93	1.39	−4.63	0.78	−0.58	0.20	−0.97	−0.19
Industrial activity land use	0.03	0.03	−0.03	0.09	0.01	0.00	0.00	0.02
Vegetation density	0.14	0.05	0.05	0.23	−0.02	0.01	−0.03	−0.00
Number of intersections	0.20	0.11	−0.02	0.42	0.03	0.02	−0.00	0.06
Segment slope	0.36	0.22	−0.07	0.80	0.04	0.03	−0.03	0.10
Random intercepts								
Day of the week								
Monday	2.47	14.41	−19.72	24.09	−0.67	0.60	−1.56	0.10
Tuesday	−29.50	14.40	−51.63	−7.70	0.27	0.59	−0.55	1.10
Wednesday	11.13	14.40	−10.89	32.92	0.16	0.58	−0.62	1.01
Thursday	15.80	14.44	−6.29	37.71	0.24	0.59	−0.56	1.13
Participant								
ID1	11.83	17.89	−14.62	38.32	0.52	1.19	−1.03	2.06
ID2	10.70	17.89	−15.78	37.26	0.19	1.19	−1.35	1.71
ID3	−22.50	17.90	−49.09	4.09	−0.69	1.19	−2.28	0.81
Temporal autocorrelation								
MA [1]	0.57	0.02	0.54	0.60	0.48	0.02	0.45	0.51
MA [2]	0.18	0.01	0.15	0.21	0.14	0.02	0.11	0.17

Second, we added nonlinear terms to control hourly systematic variation of noise and air pollution (Figure 5a,d). We expected these trends to follow road traffic patterns. For both noise and NO_2

concentration, the presence of an effect is evident. In both cases, the horizontal line represents the centered daily mean and allows us to observe when the exposure values are higher and lower during the day. For NO_2, one can distinguish three main phases. The first between 8 a.m. and 10 a.m. is characterized by a decreasing level of exposure, followed by an important rise, reaching its peak at 1:30 p.m., and finally a decrease until 7 p.m. The effect size is in the order of 20 µg/m^3 between the period with the higher and the lower concentration levels. The pattern of noise exposure is totally different. It starts with higher levels of noise at 8 a.m. and then diminishes until 2 p.m. at its lowest level. A new increase starts at 4 p.m. and seems to end at 7 p.m. These variations follow a typical road traffic pattern with first rush hours in the morning, and a second one at the end of the afternoon. Again, the size of the effect is far from negligible, with a difference of almost 2 dB(A) between the noisiest and quietest periods.

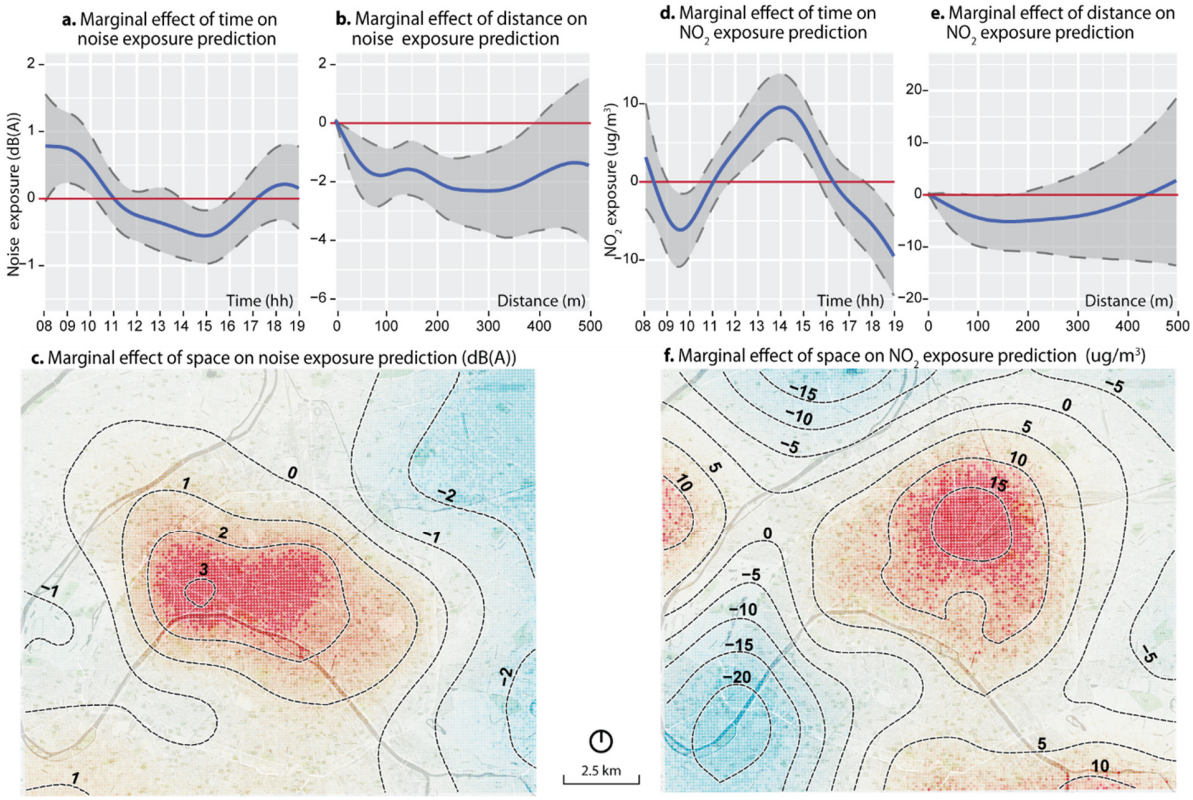

Figure 5. Marginal effects of model's nonlinear terms. Note: These maps show the splines on the geographic coordinates introduced in the model. They do not represent a concentration map for the NO_2 or noise. These spatial and temporal trends are valid only for the data collection period; they cannot be generalized over the whole year. (**a**) Marginal effect of time on noise exposure prediction; (**b**) Marginal effect of distance on noise exposure prediction; (**c**) Marginal effect of space on noise exposure prediction (dB(A)) (**d**) Marginal effect of time on NO_2 exposure prediction; (**e**) Marginal effect of distance on NO_2 exposure prediction; (**f**) Marginal effect of space on NO_2 exposure prediction (µg/m^3).

Finally, nonlinear spatial terms were introduced to control for the systematic spatial background variation of the two pollutions. They are mapped in Figure 5c,f. These maps represent the continuous functions (splines) adjusted by the model. We thus display them with a higher resolution (100 m) than the sampling resolution because of this continuous nature. Both effects are significant, with differences greater than 5 dB(A) between places with the highest and lowest levels of noise exposure, and a difference of more than 30 µg/m^3 for NO_2 exposure. The central areas, north of the Seine River, are characterized by systematically higher levels of noise and NO_2 exposure in comparison to peripheral areas. The spatial trend of NO_2 shares some similarities with the annual NO_2 concentration map proposed by AirParif in 2017 [45]. For noise, the resemblance is less pronounced, however, on both

maps, lower values of noise are discernible in the Northeast, and higher values in the 1st, 2nd, and 8th arrondissements (the principal hotspot of our spatial trend) [46]. These two spatial splines must not be interpreted as noise or air pollution concentration maps since they represent the spatial effect after controlling all the other parameters introduced in the model. They can be interpreted as a form of background pollution and are only valid for the period of the data collection, and thus must be interpreted with caution.

The main purpose of these factors in our model is to control for variation in multi-exposure not explained by the micro-scale environment and thus to obtain reliable estimates for parameters of the latter.

4.4. Micro-Scale Environment Effects

Overall, the exposure to NO_2 seems to depend less on micro-environmental characteristics than noise (Table 4) because all the coefficients except temperature have 0 in their posterior credible interval (95%). The effects are relatively weak for most of the variables. Cycling on a pedestrian street rather than a primary road could lead to a reduction of 5.7 $\mu g/m^3$ of the NO_2 exposure and cycling in a low-speed zone 1.93 $\mu g/m^3$. The canyon shape of the street seems to have little impact because of increasing the visibility of the sky by 30% would result in a reduction of NO_2 exposure of 2.1 $\mu g/m^3$. The presence of cycling infrastructure does not show any strong effect, but the exposure to NO_2 seems to be a little bit higher on lanes shared with buses (0.97 $\mu g/m^3$). The number of intersections crossed, the slope of the segment, and the density of industrial land use tend to increase the exposure to NO_2 slightly, by, respectively, 0.20 (for each supplementary intersection), 0.36 (for each point of percentage of slope), and 0.03 $\mu g/m^3$ (for each point of percentage of density). Unsurprisingly, the wind speed tends to reduce the NO_2 by 0.99 $\mu g/m^3$ for each km/h. The distance between cycling infrastructure and the nearest main street has a moderate impact on NO_2 exposure (Figure 5e). Increasing this distance could reduce the cyclists' exposure to almost 5 $\mu g/m^3$ after 100 m and the effect is not more significant after 200 m.

For noise exposure, the meteorological factors have almost no impact. For the street canyon, the model indicates that an increase of 30% of the visible sky would increase the mean noise exposure by 0.6 dB(A), suggesting that wider and more open streets are noisier. Compared to a primary street, spending 1 min on a secondary street could reduce noise exposure by 0.98 dB(A), 1.88 dB(A) for a tertiary street, 4.08 dB(A) for a residential street, 2.72 for a pedestrian street, and 1.45 dB(A) for a cycleway. Cycling on a cycle lane and on a shared cycle lane with buses tends to increase noise exposure by 0.40 and 0.52 dB(A), respectively. Opposite lanes tend to reduce cyclists' exposure by 0.63 dB(A), probably because they are usually installed on minor streets. Again, low-speed zones tend to reduce cyclists' exposure (−0.58 dB(A)), and industrial activity density tends to increase cyclists' exposure (+0.01 dB(A) for each percentage). The slope and the number of intersections encountered have a small impact on noise exposure (respectively +0.04 dB(A) and +0.03 dB(A)). Finally, the distance between cycling infrastructure and the nearest main street has a strong effect on noise exposure. A distance of 100 m could reduce the exposure to noise by almost 2 dB(A), and a weaker reduction can still be observed until 300 m (approximately 2.5 dB(A)).

5. Discussion and Limits

The main objective of this research was to investigate the impact of the micro-scale environment on cyclist' exposure to NO_2 and noise in Paris. To assess it, we realized an extensive mobile data collection and used low-cost sensors to collect data with a high space-time resolution in a high diversity of environments. Since the primary interest in this study is the role of the micro-scale environment, we used a regression model designed to remove the effect of the background pollution (random effects and nonlinear terms), temporal autocorrelation (MA2 term), and sensors' bias. The final model displays a good quality of fit, which supports the theoretical framework proposed.

5.1. O_3 Cofounding

A comprehensive assessment of the reliability of the Aeroqual Serie 500 NO_2 sensor is beyond the scope of this study, however, we would like to highlight some interesting results. We found that the temporal pattern of NO_2 exposure does not fit the traffic rush hours as expected from a pollutant essentially emitted by road traffic. This could be attributed to the cross-sensitivity of the sensor to O_3 (as discussed in Section 3.1). To investigate this result, we asked AirParif to share the data collected by their static monitoring stations during the duration of our data collection in September 2017. Figure 6a shows the daily temporal trends of NO_2 concentration for each station when controlling the day of the data collection with a generalized additive model. The impact of rush hour is clearly visible between 6 a.m. and 8 a.m. and 4 p.m. and 8 p.m. We repeated the same analysis for O_3 (Figure 6b) concentration and the sum of O_3 and NO_2 (Figure 6c). The results suggest that the temporal spline for NO_2 exposure in our model control specifically for the background O_3 concentration. Indeed, the splines of Figures 5d and 6b have a very similar shape and effect size (in the order of 20 µg/m^3). This indicates that, in our data, daily NO_2 variations caused by rush hour traffic is masked by the more pronounced temporal trend of O_3. Let us recall that we directly collected data on cyclists' exposures on the street, which differ fundamentally from regional concentration assessed by static monitoring stations. Consequently, it is not surprising to observe different trends for these two types of data.

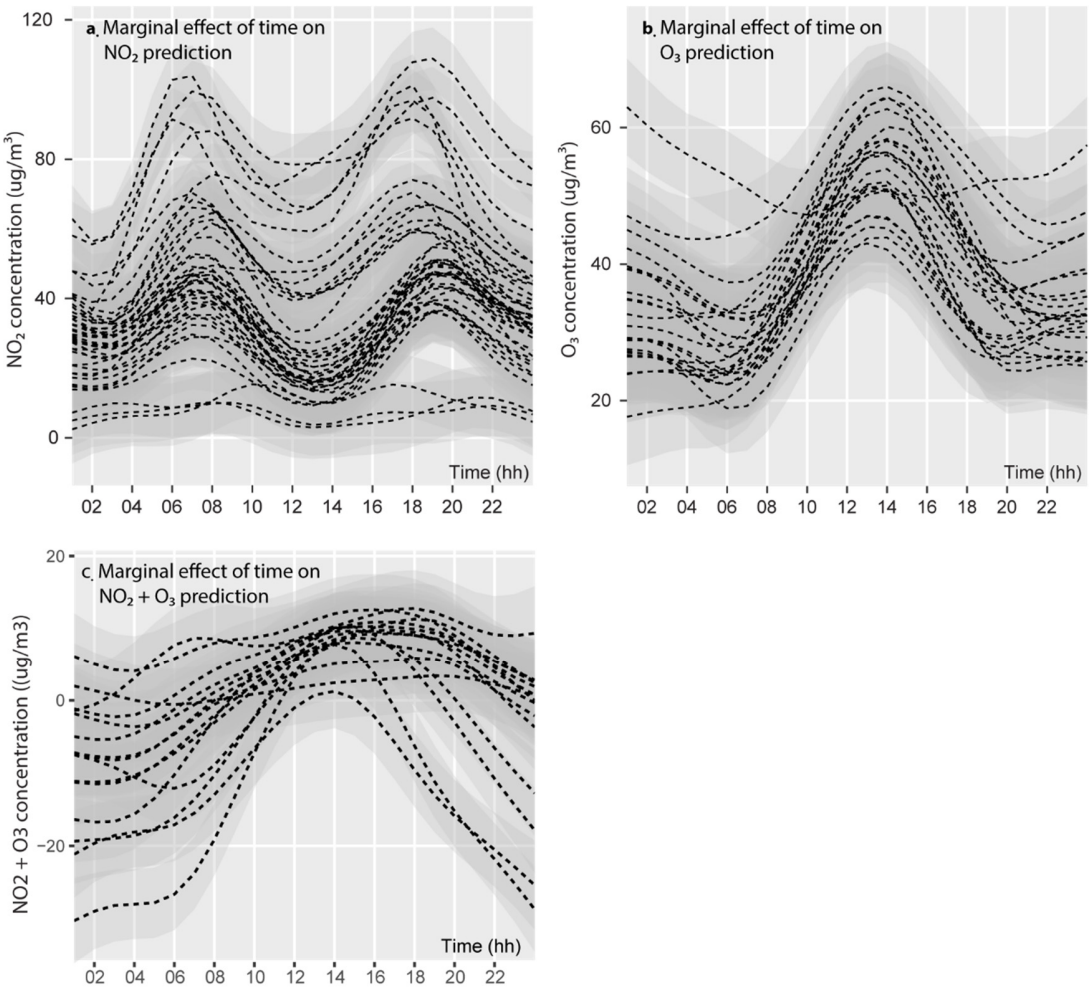

Figure 6. Modelled temporal trends of NO_2 and O_3 from AirParif monitoring stations for September 2017. (**a**) Marginal effect of time on NO_2 prediction; (**b**) Marginal effect of time on O_3 prediction; (**c**) Marginal effect of time on NO_2 + O_3 prediction

Of course, in a perfect world, a data collection using NO_2 sensors sensitive to O_3 should include an O_3 sensor to control and deduct its concentration from NO_2 as recommended by Lin et al. [60]. However, when these sensors are not available, our results suggest that the O_3 effect could be accounted for by controlling for the time of day. The intercept has a similar regulatory role in the model. It has a high value (128 $\mu g/m^3$) because it captures a significant portion of the systematic overestimation of NO_2 from the low-cost sensors. This is especially relevant in the context of monitoring with low-cost sensors because O_3 is a secondary pollutant produced when two primary pollutants react in sunlight and thus has a weak spatial variation. As a consequence, O_3 is rarely a primary interest in mobile monitoring and being able to adjust the analysis without investing in supplementary sensors could reduce the costs of such data collections. However, this result needs further investigation to determine if it holds true in other contexts.

5.2. Study Limitations

Some limitations of this study must be presented. First, our mobile data collection only covers a small temporal window and, thus, provides no information about seasonal variations of air and noise pollution exposure. It is likely that data collected during another period of the year would have yielded different results in terms of exposure. However, the direction and strength of the relations identified by the model would have probably remained similar. Second, for air pollution exposure, we only measured NO_2 but cyclists are also exposed to other air pollutants with different behaviors like particulate matter ($PM_{2.5}$, PM_{10}, black carbon, etc.). The design of the study could be replicated with additional sensors to investigate these other exposures. Third, the model presented is a Bayesian model and, therefore, influenced by the definition of the priors (presented in Supplementary Material S1). At present, we do not have enough knowledge to define informative priors, so we decided to use weakly informative and conservative priors, which might temper the results. Finally, the measured NO_2 concentration exposures probably overestimate the real exposure of cyclists in Paris because of the low-cost sensors' known limitation. As a consequence, it is difficult to determine if the cyclists' exposure levels in Paris are worrisome for health with our data. However, the statistical analysis permitted to filter out the main bias and to determine the relative effect of the environment characteristics on cyclists' exposure which is the main purpose and contribution of this study.

5.3. Implications for Planning

The weak correlation between noise and NO_2 exposure and the need to use different distributions to model them are explained by the diverse nature of these two types of pollution. Noise is an energy with an instantaneous dispersion and NO_2 is a gas that can accumulate over time. In the same way, the results suggest that NO_2 exposure is more influenced than noise by background and structural factors and, consequently, that noise is more influenced by micro-environmental characteristics.

The first consequence of this observation is that it will be more difficult to adapt planning practices to reduce cyclists' exposure to NO_2. Indeed, the factors that a planner controls (such as the type of street, vegetation, the type of cycling infrastructure, etc.) have weak effects, in the order of 0–5 $\mu g/m^3$. In contrast, for noise exposure, these factors have stronger impacts: in the order of 0.5–3 dB(A). The good news is that the effects of the micro-scale environment tend to go in the same direction for noise and NO_2. Our results indicate that cyclists are more exposed to NO_2 and noise when they are close to industrial activities, when they ride on primary roads and lanes shared with buses. In the same way, itineraries minimizing the number of intersections and riding uphill can reduce cyclists' exposure, probably because high variation in traffic speed and uphill increases motor emissions of noise and NO_2. Conversely, smaller streets, low-speed zones, and distance from main streets tend to reduce cyclists' exposure to air and noise pollution. Moreover, if we consider the spatial trends identified, it seems that the south of Paris (below the Seine river) is less marked by both types of pollution. Thus, East–West cycling infrastructure could be prioritized in this area. With regard to this last statement, it

would be necessary to repeat the study at different periods of the year to ensure that spatial trends remain similar.

Consequently, the results demonstrate that it is possible to achieve a substantial reduction in cyclists' multi-exposure by adopting new practices that include air and noise pollution dimensions in the planning of cycling infrastructure. Therefore, the development of new cycling infrastructure will reduce the current situation of transport inequity and, at the same time, encourage the use of bicycles for more sustainable cities.

5.4. Conclusions

The traditional monitoring networks are not designed to answer questions about exposures at the micro-environment scale. The mobile data collection using low-cost sensors has proven to be an interesting complementary tool, but the obtained data must be analyzed with specific statistical techniques to overcome their limitations. The growing accessibility of free data analysis software and packages makes it more and more accessible. The approach we proposed seems to produce interesting results that might be directly implemented in cycling infrastructure planning. However, this methodology must be subject to further research and should be tested in different cities. This replication work will assess the validity of the methodology and test how much the results presented are specific to Paris or could be generalized in different urban contexts.

Supplementary Materials: The following are available online at http://www.mdpi.com/2073-4433/11/4/422/s1, S1: Model priors, S2: Calculation of urban morphological indexes, S3: Posterior distributions, S4: Graphical posterior predictive checks.

Author Contributions: Conceptualization, J.G. and P.A.; Methodology and statistical analyses, J.G. and P.A.; writing—original draft reparation, J.G. and P.A.; writing—review and editing, J.G. and P.A. All authors have read and agreed to the published version of the manuscript.

Funding: This research was funded by the Canada Research Chair in Environmental Equity (950-230813) and the Fond de Recherche Société et Culture Québec.

Acknowledgments: The authors would like to thank the three anonymous reviewers for their careful reading of our manuscript and their many insightful comments and suggestions. The authors are grateful for the data complementary provided by BruitParif and AirParif.

Conflicts of Interest: The authors declare no conflict of interest.

References

1. Eriksson, C.; Pershagen, G.; Nilsson, M. *Biological Mechanisms Related to Cardiovascular and Metabolic Effects by Environmental Noise*; World Health Organization: Geneva, Switzerland, 2018.
2. Basner, M.; Babisch, W.; Davis, A.; Brink, M.; Clark, C.; Janssen, S.; Stansfeld, S. Auditory and non-auditory effects of noise on health. *Lancet* **2014**, *383*, 1325–1332. [CrossRef]
3. World Health Organization. *Environmental Noise Guidelines for the European Region*; World Health Organization: Geneva, Switzerland, 2018.
4. Brown, A.L.; Van Kamp, I. WHO environmental noise guidelines for the European region: A systematic review of transport noise interventions and their impacts on health. *Int. J. Environ. Res. Public Health* **2017**, *14*, 873. [CrossRef] [PubMed]
5. Guski, R.; Schreckenberg, D.; Schuemer, R. WHO environmental noise guidelines for the European region: A systematic review on environmental noise and annoyance. *IInt. J. Environ. Res. Public Health* **2017**, *14*, 1539. [CrossRef] [PubMed]
6. Kampa, M.; Castanas, E. Human health effects of air pollution. *Environ. Pollut.* **2008**, *151*, 362–367. [CrossRef] [PubMed]
7. World Health Organization. Ambient (Outdoor) Air Quality and Health. Available online: http://www.who.int/mediacentre/factsheets/fs313/en/ (accessed on 28 November 2017).
8. de Nazelle, A.; Bode, O.; Orjuela, J.P. Comparison of air pollution exposures in active vs. passive travel modes in European cities: A quantitative review. *Environ. Int.* **2017**, *99*, 151–160. [CrossRef]

9. Cepeda, M.; Schoufour, J.; Freak-Poli, R.; Koolhaas, C.M.; Dhana, K.; Bramer, W.M.; Franco, O.H. Levels of ambient air pollution according to mode of transport: A systematic review. *Lancet Public Health* **2017**, *2*, e23–e34. [CrossRef]
10. Okokon, E.O.; Yli-Tuomi, T.; Turunen, A.W.; Taimisto, P.; Pennanen, A.; Vouitsis, I.; Samaras, Z.; Voogt, M.; Keuken, M.; Lanki, T. Particulates and noise exposure during bicycle, bus and car commuting: A study in three European cities. *Environ. Res.* **2017**, *154*, 181–189. [CrossRef]
11. Apparicio, P.; Gelb, J.; Carrier, M.; Mathieu, M.E.; Kingham, S. Exposure to noise and air pollution by mode of transportation during rush hours in Montreal. *J. Transp. Geogr.* **2018**, *70*, 182–192. [CrossRef]
12. Observatoire des déplacements à Paris. *Le bilan des Déplacements en 2009, 2010, 2011, 2012, 2013, 2014, 2015, 2016, 2017 à Paris*; Marie de Paris: Paris, France, 2017.
13. Gössling, S. Urban transport justice. *J. Transp. Geogr.* **2016**, *54*, 1–9. [CrossRef]
14. Transport for London. Quietways. Available online: https://tfl.gov.uk/modes/cycling/routes-and-maps/quietways (accessed on 24 July 2019).
15. Künzli, N.; Kaiser, R.; Medina, S.; Studnicka, M.; Chanel, O.; Filliger, P.; Herry, M.; Horak, F.; Puybonnieux-Texier, V.; Quénel, P.; et al. Public-health impact of outdoor and traffic-related air pollution: A European assessment. *Lancet* **2000**, *356*, 795–801. [CrossRef]
16. Praznoczy, C. Les bénéfices et les risques de la pratique du vélo—Évaluation en Ile-de-France. *Pollut. Atmosphérique* **2012**, *4*, 57.
17. De Hartog, J.J.; Boogaard, H.; Nijland, H.; Hoek, G. Do the health benefits of cycling outweigh the risks? *Environ. Health Perspect.* **2010**, *118*, 1109–1116. [CrossRef] [PubMed]
18. Dekoninck, L.; Botteldooren, D.; Int Panis, L. Using city-wide mobile noise assessments to estimate bicycle trip annual exposure to Black Carbon. *Environ. Int.* **2015**, *83*, 192–201. [CrossRef] [PubMed]
19. Apparicio, P.; Carrier, M.; Gelb, J.; Séguin, A.-M.; Kingham, S. Cyclists' exposure to air pollution and road traffic noise in central city neighbourhoods of Montreal. *J. Transp. Geogr.* **2016**, *57*, 63–69. [CrossRef]
20. Hofman, J.; Samson, R.; Joosen, S.; Blust, R.; Lenaerts, S. Cyclist exposure to black carbon, ultrafine particles and heavy metals: An experimental study along two commuting routes near Antwerp, Belgium. *Environ. Res.* **2018**, *164*, 530–538. [CrossRef] [PubMed]
21. Watkins, T. *Draft Roadmap for Next Generation Air Monitoring*; Environmental Protection Agency: Washington, DC, USA, 2013; Volume 2.
22. Snyder, E.G.; Watkins, T.H.; Solomon, P.A.; Thoma, E.D.; Williams, R.W.; Hagler, G.S.; Shelow, D.; Hindin, D.A.; Kilaru, V.J.; Preuss, P.W. The changing paradigm of air pollution monitoring. *Environ. Sci. Technol.* **2013**. [CrossRef]
23. Morawska, L.; Thai, P.K.; Liu, X.; Asumadu-Sakyi, A.; Ayoko, G.; Bartonova, A.; Bedini, A.; Chai, F.; Christensen, B.; Dunbabin, M.; et al. Applications of low-cost sensing technologies for air quality monitoring and exposure assessment: How far have they gone? *Environ. Int.* **2018**, *116*, 286–299. [CrossRef]
24. Available online: https://www.epa.gov/air-sensor-toolbox/evaluation-emerging-air-pollution-sensor-performance (accessed on 24 January 2020).
25. Kumar, P.; Morawska, L.; Martani, C.; Biskos, G.; Neophytou, M.; Di Sabatino, S.; Bell, M.; Norford, L.; Britter, R. The rise of low-cost sensing for managing air pollution in cities. *Environ. Int.* **2015**, *75*, 199–205. [CrossRef]
26. Hernández-Paniagua, I.Y.; Andraca-Ayala, G.L.; Diego-Ayala, U.; Ruiz-Suarez, L.G.; Zavala-Reyes, J.C.; Cid-Juárez, S.; Torre-Bouscoulet, L.; Gochicoa-Rangel, L.; Rosas-Pérez, I.; Jazcilevich, A. Personal exposure to PM2. 5 in the megacity of Mexico: A multi-mode transport study. *Atmosphere* **2018**, *9*, 57. [CrossRef]
27. Mueller, N.; Rojas-Rueda, D.; Cole-Hunter, T.; De Nazelle, A.; Dons, E.; Gerike, R.; Goetschi, T.; Panis, L.I.; Kahlmeier, S.; Nieuwenhuijsen, M. Health impact assessment of active transportation: A systematic review. *Prev. Med.* **2015**, *76*, 103–114. [CrossRef]
28. Farrell, W.J.; Weichenthal, S.; Goldberg, M.; Hatzopoulou, M. Evaluating air pollution exposures across cycling infrastructure types: Implications for facility design. *J. Transp. Land Use* **2015**, *8*, 131–149. [CrossRef]
29. Lonati, G.; Ozgen, S.; Ripamonti, G.; Signorini, S. Variability of black carbon and ultrafine particle concentration on urban bike routes in a mid-sized city in the Po Valley (Northern Italy). *Atmosphere* **2017**, *8*, 40. [CrossRef]
30. Lioy, P.; Weisel, C. Chapter 5—Exposure Science Research Design. In *Exposure Science*; Lioy, P., Weisel, C., Eds.; Academic Press: Oxford, UK, 2014.

31. Hoek, G.; Beelen, R.; De Hoogh, K.; Vienneau, D.; Gulliver, J.; Fischer, P.; Briggs, D. A review of land-use regression models to assess spatial variation of outdoor air pollution. *Atmos. Environ.* **2008**, *42*, 7561–7578. [CrossRef]
32. Hatzopoulou, M.; Weichenthal, S.; Dugum, H.; Pickett, G.; Miranda-Moreno, L.; Kulka, R.; Andersen, R.; Goldberg, M. The impact of traffic volume, composition, and road geometry on personal air pollution exposures among cyclists in Montreal, Canada. *J. Expo. Sci. Environ. Epidemiol.* **2013**, *23*, 46. [CrossRef] [PubMed]
33. Hankey, S.; Marshall, J.D. On-bicycle exposure to particulate air pollution: Particle number, black carbon, PM2.5, and particle size. *Atmos. Environ.* **2015**, *122*, 65–73. [CrossRef]
34. MacNaughton, P.; Melly, S.; Vallarino, J.; Adamkiewicz, G.; Spengler, J.D. Impact of bicycle route type on exposure to traffic-related air pollution. *Sci. Total. Environ.* **2014**, *490*, 37–43. [CrossRef]
35. Bigazzi, A.Y.; Figliozzi, M. Roadway determinants of bicyclist exposure to volatile organic compounds and carbon monoxide. *Transp. Res. Part D Transp. Environ.* **2015**, *41*, 13–23. [CrossRef]
36. Minet, L.; Liu, R.; Valois, M.-F.; Xu, J.; Weichenthal, S.; Hatzopoulou, M. Development and Comparison of Air Pollution Exposure Surfaces Derived from On-Road Mobile Monitoring and Short-Term Stationary Sidewalk Measurements. *Environ. Sci. Technol.* **2018**, *52*, 3512–3519. [CrossRef]
37. Minet, L.; Stokes, J.; Scott, J.; Xu, J.; Weichenthal, S.; Hatzopoulou, M. Should traffic-related air pollution and noise be considered when designing urban bicycle networks? *Transp. Res. Part D Transp. Environ.* **2018**, *65*, 736–749. [CrossRef]
38. Salmond, J.A.; Williams, D.E.; Laing, G.; Kingham, S.; Dirks, K.; Longley, I.; Henshaw, G.S. The influence of vegetation on the horizontal and vertical distribution of pollutants in a street canyon. *Sci. Total. Environ.* **2013**, *443*, 287–298. [CrossRef]
39. Jereb, B.; Batkovič, T.; Herman, L.; Šipek, G.; Kovše, Š.; Gregorič, A.; Močnik, G. Exposure to black carbon during bicycle commuting–alternative route selection. *Atmosphere* **2018**, *9*, 21. [CrossRef]
40. Dekoninck, L.; Botteldooren, D.; Int Panis, L. An instantaneous spatiotemporal model to predict a bicyclist's Black Carbon exposure based on mobile noise measurements. *Atmos. Environ.* **2013**, *79*, 623–631. [CrossRef]
41. Van den Bossche, J.; De Baets, B.; Verwaeren, J.; Botteldooren, D.; Theunis, J. Development and evaluation of land use regression models for black carbon based on bicycle and pedestrian measurements in the urban environment. *Environ. Model. Softw.* **2018**, *99*, 58–69. [CrossRef]
42. Gaboriau, P. Les trois âges du vélo en France. *Vingtième Siècle. Revue d'histoire* **1991**, 17–33. [CrossRef]
43. Pucher, J.; Buehler, R.; Seinen, M. Bicycling renaissance in North America? An update and re-appraisal of cycling trends and policies. *Transp. Res. Part A Policy Pr.* **2011**, *45*, 451–475. [CrossRef]
44. Courel, J.; Riou, D.; Gouvernal, É. Le Vélo Retrouve sa Place Parmi les Mobilités du Quotidien. In *Note Rapide*; Institut d'aménagement et d'urbanisme d'île de France: Paris, France, 2014.
45. AirParif. *Bilan de la Qualité de l'air Années 2017*; AirParif: Paris, France, 2018.
46. BruitParif. *Impacts Sanitaires du Bruit des Transports dans la Zone Dense de la Région Ile-de-France*; BruitParif: Saint-Denis, France, 2019.
47. Van den Bossche, J.; Peters, J.; Verwaeren, J.; Botteldooren, D.; Theunis, J.; De Baets, B. Mobile monitoring for mapping spatial variation in urban air quality: Development and validation of a methodology based on an extensive dataset. *Atmos. Environ.* **2015**, *105*, 148–161. [CrossRef]
48. Kaur, S.; Nieuwenhuijsen, M.J.; Colvile, R.N. Fine particulate matter and carbon monoxide exposure concentrations in urban street transport microenvironments. *Atmos. Environ.* **2007**, *41*, 4781–4810. [CrossRef]
49. Marshall, J.D.; Nethery, E.; Brauer, M. Within-urban variability in ambient air pollution: Comparison of estimation methods. *Atmos. Environ.* **2008**, *42*, 1359–1369. [CrossRef]
50. Mead, M.I.; Popoola, O.; Stewart, G.B.; Landshoff, P.; Calleja, M.; Hayes, M.; Baldovi, J.J.; McLeod, M.W.; Hodgson, T.F.; Dicks, J. The use of electrochemical sensors for monitoring urban air quality in low-cost, high-density networks. *Atmos. Environ.* **2013**, *70*, 186–203. [CrossRef]
51. Shi, Y.; Lau, K.K.L.; Ng, E. Developing Street-Level PM2.5 and PM10 Land Use Regression Models in High-Density Hong Kong with Urban Morphological Factors. *Environ. Sci. Technol.* **2016**, *50*, 8178–8187. [CrossRef]
52. Steinle, S.; Reis, S.; Sabel, C.E. Quantifying human exposure to air pollution—Moving from static monitoring to spatio-temporally resolved personal exposure assessment. *Sci. Total. Environ.* **2013**, *443*, 184–193. [CrossRef]

53. Xie, S.; Zhang, Y.; Qi, L.; Tang, X. Spatial distribution of traffic-related pollutant concentrations in street canyons. *Atmos. Environ.* **2003**, *37*, 3213–3224. [CrossRef]
54. de Nazelle, A.; Fruin, S.; Westerdahl, D.; Martinez, D.; Ripoll, A.; Kubesch, N.; Nieuwenhuijsen, M. A travel mode comparison of commuters' exposures to air pollutants in Barcelona. *Atmos. Environ.* **2012**, *59*, 151–159. [CrossRef]
55. Zuurbier, M.; Hoek, G.; Oldenwening, M.; Lenters, V.; Meliefste, K.; Van Den Hazel, P.; Brunekreef, B. Commuters' exposure to particulate matter air pollution is affected by mode of transport, fuel type, and route. *Environ. Health Perspect.* **2010**, *118*, 783–789. [CrossRef]
56. Hatzopoulou, M.; Valois, M.F.; Levy, I.; Mihele, C.; Lu, G.; Bagg, S.; Minet, L.; Brook, J. Robustness of Land-Use Regression Models Developed from Mobile Air Pollutant Measurements. *Environ. Sci. Technol.* **2017**, *51*, 3938–3947. [CrossRef]
57. Gelb, J.; Apparicio, P. Noise exposure of cyclists in Ho Chi Minh City: A spatio-temporal analysis using non-linear models. *Appl. Acoust.* **2019**, *148*, 332–343. [CrossRef]
58. Dons, E.; Temmerman, P.; Van Poppel, M.; Bellemans, T.; Wets, G.; Int Panis, L. Street characteristics and traffic factors determining road users' exposure to black carbon. *Sci. Total. Environ.* **2013**, *447*, 72–79. [CrossRef]
59. Jason, T. The Challenges with Electrochemical NO2 Sensors in Outdoor Air Monitoring. Available online: https://www.aeroqual.com/challenges-electrochemical-no2-sensors-outdoor-air-monitoring (accessed on 24 January 2020).
60. Lin, C.; Gillespie, J.; Schuder, M.; Duberstein, W.; Beverland, I.; Heal, M. Evaluation and calibration of Aeroqual series 500 portable gas sensors for accurate measurement of ambient ozone and nitrogen dioxide. *Atmos. Environ.* **2015**, *100*, 111–116. [CrossRef]
61. Minet, L.; Gehr, R.; Hatzopoulou, M. Capturing the sensitivity of land-use regression models to short-term mobile monitoring campaigns using air pollution micro-sensors. *Environ. Pollut.* **2017**, *230*, 280–290. [CrossRef]
62. Delgado-Saborit, J.M. Use of real-time sensors to characterise human exposures to combustion related pollutants. *J. Environ. Monit.* **2012**, *14*, 1824–1837. [CrossRef]
63. Deville Cavellin, L.; Weichenthal, S.; Tack, R.; Ragettli, M.S.; Smargiassi, A.; Hatzopoulou, M. Investigating the use of portable air pollution sensors to capture the spatial variability of traffic-related air pollution. *Environ. Sci. Technol.* **2016**, *50*, 313–320. [CrossRef] [PubMed]
64. Huber, S.; Rust, C. Calculate travel time and distance with OpenStreetMap data using the Open Source Routing Machine (OSRM). *Stata J.* **2016**, *16*, 416–423. [CrossRef]
65. Girres, J.-F.; Touya, G. Quality Assessment of the French OpenStreetMap Dataset. *Transactions in GIS* **2010**, *14*, 435–459. [CrossRef]
66. Brovelli, M.A.; Minghini, M.; Molinari, M.E. An automated GRASS-based procedure to assess the geometrical accuracy of the OpenStreetMap Paris road network. *ISPRS Int. Arch. Photogramm. Remote. Sens. Spat. Inf. Sci.* **2016**, XLI–B7. [CrossRef]
67. Wood, S.N. *Generalized Additive Models: An Introduction with R.*; Chapman and Hall/CRC: Boca Raton, FL, USA, 2006.
68. Izenman, A.J. Multivariate Regression. In *Modern Multivariate Statistical Techniques: Regression, Classification, and Manifold Learning*; Izenman, A.J., Ed.; Springer: Berlin/Heidelberg, Germany, 2008; pp. 159–194.
69. R Core Team. *R: A language and Environment for Statistical Computing*; R Foundation for Statistical Computing: Vienna, Austria, 2019.
70. Bürkner, P.-C. Advanced Bayesian Multilevel Modeling with the R package Brms. *arXiv* **2017**, arXiv:1705.11123. [CrossRef]
71. Carpenter, B.; Gelman, A.; Hoffman, M.D.; Lee, D.; Goodrich, B.; Betancourt, M.; Brubaker, M.; Guo, J.; Li, P.; Riddell, A. Stan: A probabilistic programming language. *J. Stat. Softw.* **2017**, *76*. [CrossRef]
72. Merritt, A.-S.; Georgellis, A.; Andersson, N.; Bedada, G.B.; Bellander, T.; Johansson, C. Personal exposure to black carbon in Stockholm, using different intra-urban transport modes. *Sci. Total. Environ.* **2019**, *674*, 279–287. [CrossRef]
73. Boogaard, H.; Borgman, F.; Kamminga, J.; Hoek, G. Exposure to ultrafine and fine particles and noise during cycling and driving in 11 Dutch cities. *Atmos. Environ.* **2009**, *43*, 4234–4242. [CrossRef]
74. Davies, H.W.; Vlaanderen, J.; Henderson, S.; Brauer, M. Correlation between co-exposures to noise and air pollution from traffic sources. *Occup. Environ. Med.* **2009**, *66*, 347–350. [CrossRef]

75. Sueur, J.; Aubin, T.; Simonis, C. Seewave, a free modular tool for sound analysis and synthesis. *Bioacoustics* **2008**, *18*, 213–226. [CrossRef]
76. OpenStreetMap. Key: Highway. Available online: https://wiki.openstreetmap.org/wiki/Key:highway (accessed on 24 January 2020).